metals

MDPI

Communication

Low-Temperature Induced Martensitic Transformation Enhancing Mechanical Properties of Metastable Fe-Ni-P Alloy

Guodong Cui *, Runjian Jiang, Chengsong Zhang and Yuxuan Liu

School of Materials Science and Engineering, Southwest Jiaotong University, Chengdu 610031, China
* Correspondence: gdcui@swjtu.edu.cn; Tel.: +86-136-8848-1468

Received: 15 June 2019; Accepted: 13 July 2019; Published: 14 July 2019

Abstract: The metastable Fe-Ni-P alloy with phosphorus (P) solid-solution structure has been fabricated by spark plasma sintering. Its face-centered cubic (FCC) matrix without the precipitation of phosphide attains a high plasticity and an excellent strain hardening ability at room temperature. This Fe-Ni-P alloy is subjected to cryogenic treatment at various temperatures (−20 °C and −50 °C), to investigate the role of phosphorus on the microstructural evolution and mechanical properties of γ-(Fe-Ni) alloy at low temperatures. The results indicate that the addition of phosphorus can destabilize the Fe-Ni-P alloy and facilitate its martensitic transformation during cryogenic treatment. P-doping does not lead to obvious embrittlement of Fe-Ni-P alloy at low temperatures, but strengthens the alloy by promoting microstructure evolution. The Fe-Ni-P alloy has high plasticity and good strain hardening ability after treated at −20 °C, and is converted to acicular martensite structure after being treated at −50 °C, resulting in a significant increase in its hardness (433 HV) and compressive yield strength (1271 MPa). Developing this Fe-Ni-P alloy as a load-bearing component for low-temperature conditions shows great promise.

Keywords: metastable Fe-Ni-P alloy; cryogenic treatment; martensitic transformation; microstructure; mechanical characterization

1. Introduction

As reported in many steels, including austenitic stainless steel, interstitial free steel (IF steel) and high phosphorus steel (HPS) [1,2], doping a small amount of phosphorus is a feasible way to improve the mechanical properties of high-strength steels for engineering. In addition, the microstructural transformations can also be observed after P is doped into some sintered alloys like Fe-P, Fe-P-Cr and Fe-Ni-P alloys [3–5]. However, P is conventionally seen as an impurity element, since its segregation to grain boundaries can lead to the embrittlement of steels at low temperatures [6,7]. As the temperature decreases, so too does the plasticity of steels. For decades, controlling this deleterious effect has been a topic of great concern to the material science community.

Recently a kind of α-(Fe-Ni-P) alloy has been developed by the semi-liquid phase sintering of Fe-Ni-P composite powders [5,8]. The doping of P facilitates the sintering process by promoting the formation of semi-liquid Ni-P phase during sintering, and the precipitated bulk phosphide phase can also strengthen the alloy. However, its plasticity is not ideal due to the matrix with body-centered cubic (BCC) structure. The segregation of P to grain boundary also leads to the reduction in its ability to resist deformation at low temperatures [8]. It is reported that increasing P content is a cause for the increased ductile-brittle transition temperature (DBTT) of α-(Fe-Ni) based alloys, and this may restrict the applications of such alloy at low temperatures [9,10]. However, the Fe-Ni based alloys with FCC structure possess excellent plasticity. We would like to utilize this feature of FCC structure

in order to achieve the strengthening effect of P on this γ-(Fe-Ni-P) alloy without obvious increase of its DBTT. The cold shortness phenomenon is devastating for α-(Fe,Ni) alloy, whereas the embrittlement caused by this phenomenon can be weakened in γ-(Fe,Ni) alloy [11,12]. In fact, P has a much higher solubility in the FCC lattice of γ-(Fe,Ni) alloy. This is able to contribute to an uniform distribution of P in the γ-(Fe,Ni-P) alloy and also to inhibit its segregation to the grain boundaries. Therefore, a phosphorus solid-solution structure can be developed in γ-(Fe-Ni-P) alloy; and P can work as a strengthening element in this alloy at low temperatures, rather than causing the grain boundary embrittlement. The role of phosphorus in γ-(Fe-Ni-P) alloys are rarely reported in recent literature; and investigation on the microstructure and mechanical properties of γ-(Fe-Ni-P) alloy at a low temperature is of great implication for materials design.

In this paper, the metastable γ-(Fe-Ni-P) alloys with the phosphorus solid-solution structure is fabricated by spark plasma sintering (SPS) facility. To understand the performance of P-contained γ-(Fe-Ni) alloys at low temperatures, they have been subjected to cryogenic treatment. Phosphorus, as a ferrite stabilizer, can decrease the stability of γ-(Fe-Ni-P) alloys, and can promote their transformation during cryogenic treatment. Therefore, influences of treatment temperature on the microstructure and mechanical properties of metastable γ-(Fe-Ni-P) alloys have been studied and analyzed.

2. Materials and Methods

2.1. Synthesis Process

Commercial carbonyl iron powder (99.5% purity and 5 μm in average size) was used as raw material in this work. It was added into electroless plating solution and then heated in the thermostat water bath in order to prepare the Fe-Ni-P composite powder. Electroless plating solution mainly consisted of $NiSO_4 6H_2O$ (main salt; 30 g/L) and $NaH_2PO_2H_2O$ (reducing agent; 25 g/L) and its pH value was regulated to 6 by ammonia water. The content of Ni-P coating was precisely adjusted to 30 wt.% by controlling the plating temperature (70 °C). According to Fe-Ni phase diagram [13], such high Ni content is of benefit to obtain FCC structure in samples. After electroless plating process, the composite powders were filtered out and were washed by ethanol for three times. Then, they were dried in the vacuum drying box at 35 °C for 24 h.

Then, the as-prepared Fe-Ni-P composite powders were packed in a graphite die with an inner diameter of 20 mm and a height of 60 mm. They were compacted under the load of 9.36 MPa (300 kg) to get the green compact. The specimens were fabricated in a spark plasma sintering (SPS) machine (Sumitomo Coal Mining Company Model 1050, Sumitomo, Tokyo, Japan) with a vacuum condition $<10^{-3}$ Pa. The specimens were heated to 875 °C with a heating rate of 200 °C min^{-1} and held for 5 min, followed by furnace cooling in vacuum. An external stress of 20 MPa was maintained throughout the sintering process. The Fe-Ni-P alloys (ϕ20 × 35 cylinder) with a composition of 68.1 wt.% Fe-31.2 wt.% Ni-0.6 wt.% P and a density of 8.1 g cm^{-3} were prepared. Then, those sintered γ-(Fe-Ni-P) alloys were subjected to cryogenic treatment at different temperature. They were put into ethanol/liquid-nitrogen solution for 10 min at −20 °C and −50 °C respectively. Finally, the treated specimens were taken out and dried. Three groups of Fe-Ni-P alloys with different treatment routes have been described: the sintered alloy (20 °C; named S-RT), followed by cryogenic treatment at −20 °C (named S-CT1), and at −50 °C (named S-CT2).

2.2. Characterization

These Fe-Ni-P alloys were cut into cylinders of ϕ10 × 15 mm for compressive performance test on the electronic universal testing machine (WDW-200) with a strain rate of 0.5 mm/min. At least three samples from each group of alloy were used for mechanical property test. The apparent yield properties were determined using the 0.2% offset method. The Vickers hardness (HV) of alloys were measured with a digital micro-hardness tester (HVS-1000 B, Huayin, Laizhou, China) at a load of 0.98 N and a dwell time of 15 s. The hardness values were obtained by averaging 10 measurements selected randomly on the specimens. The alloy compositions were measured by X-ray fluorescence

spectrometer (XRF, X-MET7500, Oxford Instruments, Abingdon-on-Thames, UK). The phase structures were characterized by X-ray diffraction (XRD) with Cu Kα radiation (X' pert pro XRD, PANalytical Co., Almelo, The Netherlands). The Bragg angles were adjusted in the range of 30–90° for the samples with a scanning rate of 5°/min. The micrographs of specimens were determined by desktop scanning electron microscope (pro G2, Phenom world, Eindhoven, The Netherlands). The elemental distributions of specimens were observed in field emission scanning electron microscopy (FE-SEM, JSM-7001F, JEOL, Tokyo, Japan) equipped with an energy-dispersive X-ray spectrometer (EDS).

3. Results and Discussion

3.1. Microstructures of Metastable Fe-Ni-P Alloys after Cryogenic Treatment

The X-ray diffraction patterns (XRD) showing phase structures of Fe-Ni-P alloys are displayed in Figure 1, together with the standard patterns of α-Fe and γ-Fe. There is only one series of peaks corresponding to α-Fe on the XRD pattern of Fe-Ni-P powder, and the characteristic peaks of Ni-P coating are absent. This is because the Ni-P coating prepared via electroless plating is thin and in amorphous state [14,15]. The phase structures consisting of γ-(Fe-Ni-P) and α-(Fe-Ni-P) are found in Fe-Ni-P alloys after SPS process. The formation of γ-phase is promoted by the diffusion of Ni, an austenite stabilizer, into Fe matrix during the sintering [16]. Compared with those in raw Fe-Ni-P powders, the much larger peak width of α-phase and γ-phase in sintered Fe-Ni-P alloys indicates that a large number of P atoms have dissolved into the matrix during the sintering. As a result, a phosphorus solid-solution structure forms in these Fe-Ni-P sintered alloys. It is noted that these Fe-Ni-P sintered alloys can be considered to be metastable, and a low temperature can induce the martensitic transformation of γ-(Fe-Ni-P) phase to α-(Fe-Ni-P) phase. As a ferrite stabilizer, phosphorus will increase the destabilization of this γ-(Fe-Ni-P) phase when it is in a solid-solution state and causes lattice distortion of the γ-phase. Therefore, martensitic transformation in this γ-(Fe-Ni-P) phase is more prone to occur at a low-temperature condition. The proportion of γ-phase in each alloy decreases significantly with decreasing the treatment temperature, and the phase structure of Fe-Ni-P alloy is almost completely converted to α-phase when it is treated at −50 °C.

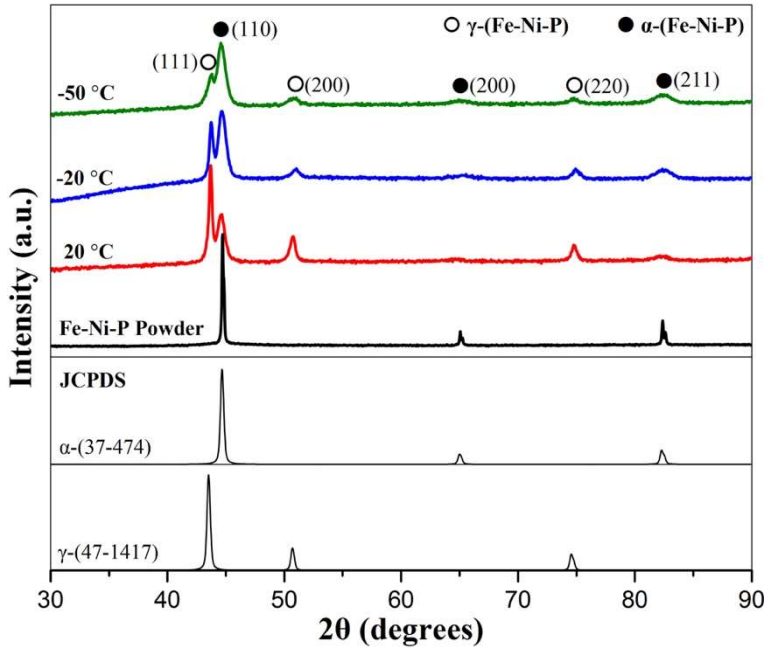

Figure 1. XRD patterns of Fe-Ni-P powder, Fe-Ni-P alloys before/after cryogenic treatment.

Moreover, compared with standard patterns, the peak shifts are found in Fe-Ni-P alloys after the cryogenic treatment. The lattice distortions of γ-(Fe-Ni-P) phase and α-(Fe-Ni-P) phase can be

evaluated from these shifts of their respective main peaks. The calculations show that with decreasing the treatment temperature, cubic lattice parameter of γ-(Fe-Ni-P) phase decreases from 3.584 Å to 3.576 Å, and cubic lattice parameter of α-(Fe-Ni-P) phase increases from 2.867 Å to 2.873 Å. This phenomenon indicates that in alloys after cryogenic treatment (alloy S-CT1 and S-CT2), the lattice expansion of α-(Fe-Ni-P) phase becomes severer, while the lattice distortion of γ-(Fe-Ni-P) phase has been weakened (3.516 Å for standard γ-(Fe-Ni) lattice). The P atom is the primary cause of the lattice distortions in Fe-Ni matrix. The difference in lattice distortion between these two phases illustrates that P trends to solid solution in the α-(Fe-Ni-P) phase, rather than residual γ-(Fe-Ni-P) phase. In these alloys after cryogenic treatment, such α-(Fe-Ni-P) phase comes from the martensitic transformation of previous γ-(Fe-Ni-P) phase. Therefore, it can be inferred that the γ-(Fe-Ni-P) phase with a phosphorus solid-solution structure in this metastable Fe-Ni-P alloy is more prone to undergo martensitic transformation at low temperatures.

Figure 2 shows the optical microscope (OM) images of the cross-sections of three groups of Fe-Ni-P alloys. They were etched by $CuSO_4$/hydrochloric acid/alcohol solution, to clearly show the grain boundaries and the interfaces. The Fe-Ni-P alloy prepared by SPS process (S-RT) is fully dense with a microstructure composed of γ-phase and α-phase (see Figure 2b, 20 °C); and each grain in this alloy contains both phases. Through quantitative metallography method, it is determined that the volume fractions of γ-phase and α-phase are about 75% and 25% respectively. Compared with conventional sintering, spark plasma sintering provides the alloy S-RT with a much coarser grain size and less precipitated phosphide [5]. Figure 2b clearly demonstrates the dissolution of P atoms into alloy matrix and the formation of a phosphorus solid-solution structure during the SPS process. However, the microstructure of Fe-Ni-P alloys has transformed significantly after the cryogenic treatment. When the temperature decreases to −20 °C, the γ-(Fe-Ni-P) phase in alloy is partially converted to α-(Fe-Ni-P) phase. It is noted that such α-phase is nucleated from the inside of γ-phase grains and grows in a certain direction to form a finer acicular structure. When the temperature further decreases to −50 °C, the Fe-Ni-P alloy consists of α-(Fe-Ni-P) phase and a few γ-(Fe-Ni-P) phase. The volume fractions of α-(Fe-Ni-P) phase in these alloys are determined to be 65% at −20 °C and 90% at −50 °C respectively. As seen in Figure 2d,f, the α-(Fe-Ni-P) phase in alloys after cryogenic treatment can be identified as acicular martensite.

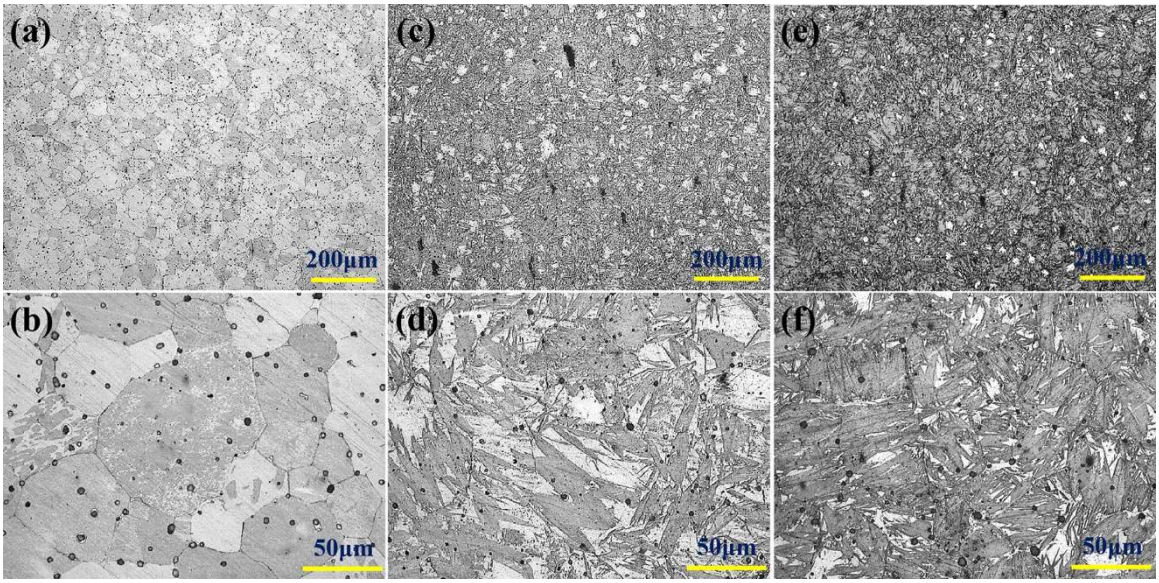

Figure 2. Microstructure of Fe-Ni-P alloys before/after cryogenic treatment: (**a**,**b**) 20 °C; (**c**,**d**) −20 °C; (**e**,**f**) −50 °C.

The rapid thermal diffusion of phosphorus greatly improves its dissolution in γ-(Fe-Ni) matrix during the SPS process. In return, the resulted microstructure in Fe-Ni-P alloy can be metastable and the martensitic transformation of γ-(Fe-Ni-P) phase can be easily triggered at low temperatures.

Generally, low-temperature induced martensitic transformation in conventional γ-(Fe-Ni) alloys occurs at near boiling nitrogen temperature [17]. In the alloys with a phosphorus solid-solution structure, the phosphorus atom, one with a larger atomic radius, is located in the octahedral gap of FCC lattice of γ-(Fe-Ni) matrix. This leads to the expansion of matrix lattice and the shift of Fe/Ni atoms towards the center of adjacent lattice. As a result, the strain energy of FCC lattice of γ-(Fe-Ni-P) phase increases greatly. When this metastable Fe-Ni-P alloy is subjected to cryogenic treatment, the matrix lattice tends to be stabilized and correspondingly reduce its strain energy to minimum. Therefore, the shifted Fe/Ni atoms prefer to occupy the body center of the neighboring lattice during cryogenic treatment and BCC lattice of α-(Fe-Ni-P) phase forms. Under this circumstance, this phosphorus solid-solution structure destabilizes the γ-(Fe-Ni-P) phase, and the martensite transformation in this metastable Fe-Ni-P alloy is more prone to occur at low temperatures.

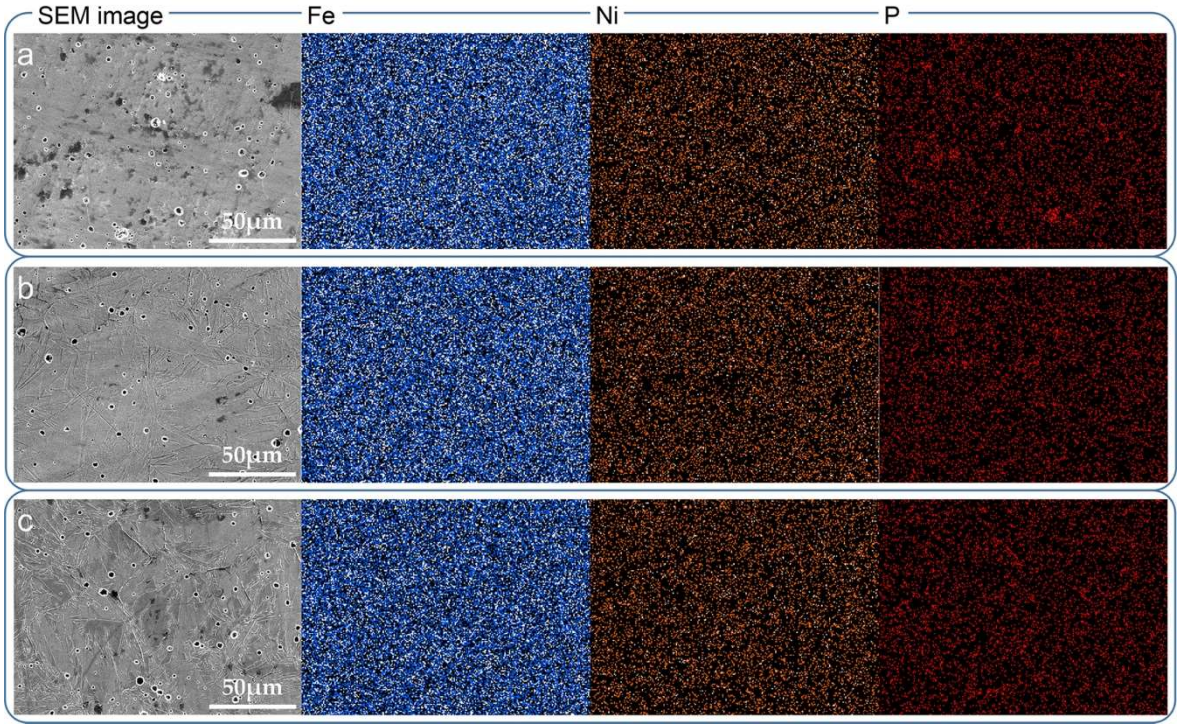

Figure 3. Energy-dispersive X-ray spectrometer (EDS) surface mapping showing the composition distribution of Fe-Ni-P alloys before/after cryogenic treatment: (**a**) 20 °C; (**b**) −20 °C; (**c**) −50 °C.

The surface chemical composition mappings of three groups of Fe-Ni-P alloys are displayed in Figure 3. As described above, the microstructure transformation of Fe-Ni-P sintered alloys after cryogenic treatment is remarkable, but the distribution features of their major compositions have not changed significantly. In the Fe-Ni-P alloy after SPS process (alloy S-RT), Fe and Ni have a uniform distribution. There is no evidence of the formation of phosphide in the P mapping of this alloy, and the segregation of phosphorus to grain boundaries is also not observed. This, in accordance with previous observations, has confirmed the formation of phosphorus solid-solution structure in Fe-Ni-P sintered alloy. During cryogenic treatment, Fe and Ni in alloy S-CT1 and S-CT2 did not diffuse and redistribute, and only the transition of γ-phase to α-phase occurred. It should be noted that even at low temperatures, the P mappings still show a uniform distribution and a solid-solution state in matrix. The cryogenic treatment does not result in the segregation of phosphorus at the grain boundaries, and therefore the grain boundary embrittlement of this Fe-Ni-P sintered alloy is avoided at low temperatures. It can be seen from Figure 3 that this low-temperature induced martensitic transformation in metastable Fe-Ni-P sintered alloys has little to no impact on their composition distribution, even though their morphology and phase structure has changed. This is because during martensitic transformation—a type of non-diffusion phase transition—the atoms in Fe-Ni-P alloys

are displaced through shearing rather than migration, and the new phase (α-phase) possesses the same chemical composition as the previous phase (γ-phase).

3.2. Mechanical Properties of Metastable Fe-Ni-P Alloys after Cryogenic Treatment

The compression performance of metastable Fe-Ni-P alloys after cryogenic treatment are investigated in order to clarify the benefits of low-temperature martensitic transformation. Figure 4a shows the selected compressive stress–strain curves of Fe-Ni-P alloys at a strain rate of 1.5×10^{-3} s^{-1}, and Table 1 lists their specific mechanical properties data. The alloy S-RT (20 °C) exhibits high plasticity and excellent deformation strengthening ability (Figure 4b). This strain hardening can contribute to the improvement of this Fe-Ni-P sintered alloy's ability to withstand external loads. It is noted that even though alloy S-RT undergoes severe plastic deformation when applied with a compressive stress exceeding 4 GPa, there is still no obvious crack initiation on its surface. This alloy has a Vickers micro-hardness of 262 HV and a yield strength of 608 MPa. The solid-solution strengthening of phosphorus in matrix and the presence of a small amount of α-phase jointly contribute to the good hardness and strength of this Fe-Ni-P sintered alloy.

Table 1. The mechanical properties data of Fe-Ni-P alloys with different treatment routes.

Temperature (°C)	Hardness ($HV_{0.1}$)	Young's Modulus (GPa)	Yield Strength (MPa)	Maximum Stress (MPa)	Maximum Strain (%)
20	262 ± 21	15.5	608	4151	67
−20	354 ± 32	15.8	716	3880	70
−50	433 ± 27	17.5	1271	2010	31

A significant enhancement in the mechanical properties of Fe-Ni-P alloys is observed due to the martensitic transformation occurring in cryogenic treatment. The alloy S-CT1 has an obviously increased hardness of 354 HV and yield strength of 716 MPa, while it still has a good plasticity (see Figure 4a). Its excellent mechanical property is because of the presence of a large amount of γ-(Fe-Ni-P) phase with a phosphorus solid-solution structure and the martensite strengthening induced by low temperature [18]. The good strain hardening ability similar to alloy S-RT is also found in this alloy after cryogenic treatment at −20 °C (see Figure 4b). This is because of the working hardening and the martensitic transformation during the plastic deformation of Fe-Ni-P alloy. The highly plastic γ-phase has a high proportion in alloys treated at 20 °C and −20 °C. This P-contained γ-phase has a considerable strength and better plastic deformation ability. It can also be strengthened by deformation-induced martensitic transformation. Therefore, there is an increase in strain hardening rates of alloy S-RT and alloy S-CT1. In fact, the precipitation of phosphide is a dynamic process that is dependent on sintering time and temperature, and the conventional sintering process can provide favorable conditions for its formation [19,20]. However, in this Fe-Ni-P alloy prepared by SPS process, a higher heating rate and a lower sintering temperature make the semi-liquid Ni-P phase to exist temporarily during the sintering process. Hence, there is no precipitation of phosphide, but the formation of highly plastic γ-(Fe-Ni-P) phase [21,22]. It is noted that even if the crack has initiated in the surface (marked in Figure 4b), the alloy S-CT1 is still able to withstand higher stress and continue to deform, rather than breaking immediately. This metastable Fe-Ni-P alloy can be applied to the load-bearing parts at high latitude areas, since this phenomenon is regarded as a signal that provides an early warning for the occurrence of catastrophic accidents. In contrast, the deformation behaviour of alloy S-CT2 is characterized by a typical brittle mode, since most of γ-(Fe-Ni-P) phase has been transformed into α-(Fe-Ni-P) phase at −50 °C. Its hardness and yield strength have reached 433 HV and 1271 MPa respectively, but its strain to failure has decreased to 31%. A slight increase in strain hardening rate is observed during the plastic deformation stage of Fe-Ni-P alloy after cryogenic treatment at −50 °C (arrow "A" in Figure 4b), and this is perhaps because of the deformation-induced transformation of residual γ-phase to α-phase [23]. Overall, the strength of this metastable Fe-Ni-P alloy increases as temperature decreases. It is concluded that phosphorus in solid-solution state can

strengthen the Fe-Ni-P sintered alloy at low temperatures by promoting the martensitic transformation.

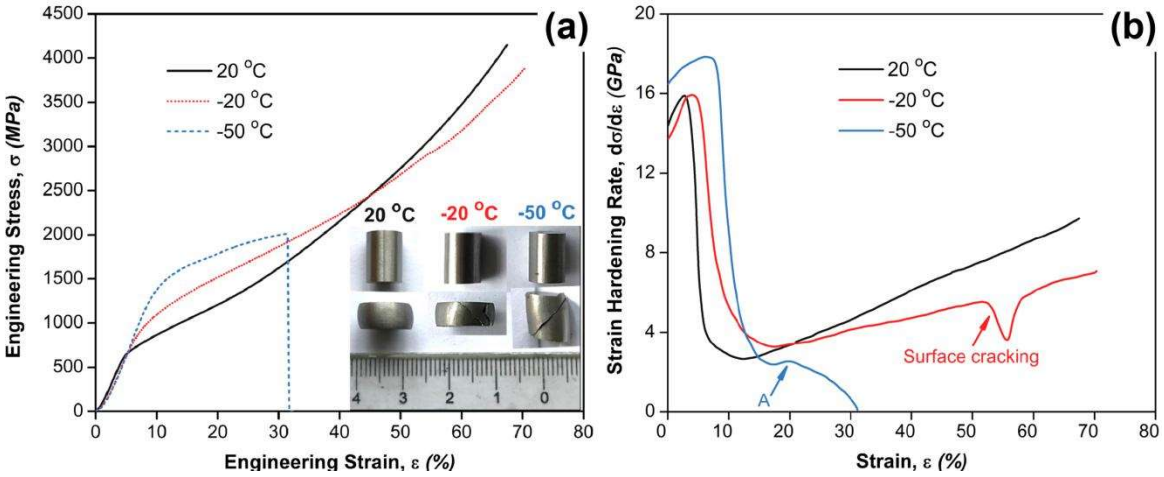

Figure 4. Compressive strain-stress curves (**a**) and strain hardening rate vs strain curves (**b**) of Fe-Ni-P alloys before/after cryogenic treatment.

4. Conclusions

With the assistance of spark plasma sintering, the phosphorus solid-solution structure is developed in Fe-Ni-P alloy and the precipitation of brittle phosphide is suppressed. Phosphorous in solid-solution state facilitates the martensitic transformation in this metastable Fe-Ni-P alloy during the cryogenic treatment, and the cold shortness effect is not obvious. This low-temperature induced martensitic transformation not only contributes to the formation of acicular martensite structure, but also leads to a remarkable improvement in hardness (433 HV) and yield strength (1271 MPa) of this Fe-Ni-P alloy at −50 °C. The main contribution in the present work is a demonstration that, at a low temperature, phosphorus in solid-solution state is capable of enhancing the strength of metastable Fe-Ni-P alloy without significantly sacrificing its plasticity. This paper is expected to have a guiding importance for the design of phosphorus-doped ferroalloys.

Author contributions: G.C. prepared original draft; R.J. reviewed and edited; G.C. initiated the research and provided technical input; R.J. and Y.L. prepared samples and performed experimental operations; R.J., G.C. and C.Z. contributed to the technical discussions of results. All the authors commented on the manuscript.

Funding: This research was funded by the National Natural Science Foundation of China, grant number 51601156 and the APC was funded by Guodong Cui.

Conflict of Interests: The authors declare no conflicts of interest.

References

1. Santos, A.P.R.; Mota, T.C.; Segundo, H.V.G.; Almeida, L.H.; Araújo, L.S.; Rocha, A.C. Texture, microstructure and anisotropic properties of IF-steels with different additions of titanium, niobium and phosphorus. *J. Mater. Res. Technol.* **2018**, *7*, 331-336.
2. Katiyar, A.K.; Rajput, S.K.; Mehta, Y. Microstructural Evolution of High Phosphorus Steel Using Warm Multiaxial Deformation. *Mater. Today Proc.* **2017**, *4*, 9380-9383.
3. Muthuchamy, A.; Kumar, R.; Annamalai, A.R.; Agrawal, D.K.; Upadhyaya, A. An investigation on effect of heating mode and temperature on sintering of Fe-P alloys. *Mater. Charact.* **2016**, *114*, 122-135.
4. Trivedi, S.; Mehta,Y.; Chandra, K.; Mishra, P.S. Effect of chromium on the mechanical properties of powder-processed Fe-0.45 wt.% P alloys. *J. Mater. Process. Tech.* **2010**, *210*, 85-90.
5. Chai, W.; German, R.M.; Olevsky, E.A.; Wei, X.; Jiang, R.; Cui, G. Preparation and Properties of High Strength Fe-Ni-P Ternary Alloys. *Adv. Eng. Mater.* **2016**, *18*, 1889-1896.
6. Grabke, H.J.; Moller, R.; Erhart, H.; Brenner, S.S. Effects of the Alloying Elements Ti, Nb, Mo and V on the Grain Boundary Segregation of P in Iron and Steels. *Surf. Interface Anal.* **1987**, *10*, 202-209.

7. Zhong, L.; Wu, R.; Freeman, A.J.; Olson, G.B. Effects of Mn additions on the P embrittlement of the Fe grain boundary. *Phys. Rev. B* **1997**, *55*, 11133.
8. Jiang, R.; Li, A.; Cui, G.; Zhang, C.; Chen, H.; Wang, Y. Influence of Ni-P content on microstructure and mechanical properties of Fe-x(Ni+P)-1Cu alloys. *Mater. Sci. Eng. A* **2017**, *707*, 1-11.
9. Song, S.H.; Zhuang, H.; Wu, J.; Weng, L.Q.; Yuan, Z.X.; Xi, T.H. Dependence of ductile-to-brittle transition temperature on phosphorus grain boundary segregation for a 2.25Cr1Mo steel. *Mater. Sci. Eng. A* **2008**, *486*, 433-438.
10. Kameda, J.; Nishiyama, Y. Combined effects of phosphorus segregation and partial intergranular fracture on the ductile-brittle transition temperature in structural alloy steels. *Mater. Sci. Eng. A* **2011**, *528*, 3705-3713.
11. Danilchenko, V.; Dzevin, I.; Sagaradze, V. Effect of Multiple Martensitic Transformations on Structure of Fe-Ni Alloys. *J. Mater. Sci. Technol.* **2013**, *29*, 279-282.
12. Chen, Z.; Chen, Q.; Liu, F.; Yang, X.Q.; Fan, Y.; Zhang, C.H.; Liu, A.M. The influence of solid-state grain growth mechanism on the microstructure evolution in undercooled Ni-10 at.% Fe alloy. *J. Alloy. Compd.* **2015**, *622*, 1086-1092.
13. Swartzendruber, L.J.; Itkin, V.P.; Alcock, C.B. The Fe-Ni (iron-nickel) system. *J. Phase Equilib.* **1991**, *12*, 288-312.
14. Zhan, X.; Ernst, F. Crystallization micro-mechanism of near-eutectic amorphous Ni-P. *Acta Mater.* **2016**, *104*, 274-282.
15. Krishnan, K.H.; John, S.; Srinivasan, K.N.; Praveen, J.; Ganesan, M.; Kavimani, P.M. An overall aspect of electroless Ni-P depositions-A review article. *Metall. Mater. Trans. A* **2006**, *37*, 1917-1926.
16. Shongwe, M.B.; Diouf, S.; Durowoju, M.O.; Olubambi, P.A. Effect of sintering temperature on the microstructure and mechanical properties of Fe-30% Ni alloys produced by spark plasma sintering. *J. Alloy. Compd.* **2015**, *649*, 824-832.
17. Shirazi, H.; Miyamoto, G.; Nedjad, S.H.; Chiba, T.; Ahmadabadi, M.N.; Furuhara, T. Microstructure evolution during austenite reversion in Fe-Ni martensitic alloys. *Acta Mater.* **2018**, *144*, 269-280.
18. Niessen, F.; Villa, M.; Somers, M.A.J. Martensite Formation from Reverted Austenite at Sub-zero Celsius Temperature. *Metall. Mater. Trans. A* **2018**, *49*, 5241-5245.
19. Chan, T.; Lin, S. Injection molding of Fe-Ni-P composite powders prepared by electroless nickel plating and the magnetic properties of the sintered alloys. *J. Mater. Process. Tech.* **1999**, *89-90*, 165-170.
20. Chan, T.Y.; Lin, S.T. Enhanced sintering of an Fe-Ni-P coated composite powder prepared by electroless nickel plating. *JMEPEG* **1997**, *6*, 628-632.
21. Bousnina, M.A.; Turki, F.; Schoenstein, F.; Tetard, F.; Rabu, P.; Smiri, L.S.; Jouini, N. Bulk nanostructured Ni-P alloys: Elaboration from metastable Ni-P nanoparticles by spark plasma sintering; mechanical and magnetic properties. *J. Alloy. Compd.* **2016**, *686*, 252-266.
22. Jiang, R.; Li, A.; Cui, G.; Zhang, C. Comparison of Microstructure and Mechanical Properties of Sintered γ-(Fe-Ni-P) Alloys with Abundant P Doping. *Metall. Mater. Trans. A* **2019**, *50*, 2580-2584.
23. Guimaraes, J.R.C.; Rios, P.R. The mechanical-induced martensite transformation in Fe-Ni-C alloys. *Acta Mater.* **2015**, *84*, 436-442.